# Photon-Timing Detector Module for Single-Molecule Spectroscopy With 60-ps Resolution

Ivan Rech, Guobin Luo, Massimo Ghioni, *Member, IEEE*, Haw Yang, Xiaoliang Sunney Xie, and Sergio Cova, *Fellow, IEEE*

*Abstract*—Advanced fluorescence measurements on single molecules demand single-photon detectors with high-quantum detection efficiency, low noise, and high time resolution. We have developed a compact ($82 \times 60 \times 30$ mm) and versatile single-photon timing module (SPTM), based on a planar epitaxial single photon avalanche diodes (SPAD) working with a monolithic integrated active quenching and active reset circuit (i-AQC) and cooled by a Peltier element. The main operating parameters are computer controlled via RS-232 interface and the photon counting rate can be continuously monitored. The photon detection efficiency is 45% at 500 nm with cooling at $-15\ ^{\circ}$C, the dark counting rate is 5 c/s with SPAD operating at 5 V excess bias voltage, 10 c/s operating at 10 V. The time resolution obtained with tightly focused illumination has 60-ps full-width at half-maximum. Comparative tests with the SPTM prototype and with an advanced commercially available photon counting module confirmed that the time resolution and sensitivity of the SPTM make it possible to resolve and measure even short lifetime components of a single molecule. The SPTM thus made possible experiments leading to a deeper insight into angstrom-scale structural changes of single-protein molecules.

*Index Terms*—Avalanche photodiode, picosecond timing, single molecule, single photon, single-photon timing module (SPTM).

## I. INTRODUCTION

THE single-molecule approach has changed the way biophysical and biochemical problems are addressed, and new insights derived from the approach are continuously emerging due to the effort of many research groups. Many experimental studies rely on detecting and measuring the fluorescent emission of a single molecule, a task that sets severe requirements to the photon detector. For attaining an adequate signal-to-noise ratio, both high-quantum detection efficiency (QE) and low noise (i.e., low dark counting rate) are necessary. The QE of solid-state detectors is inherently superior to that of photomultiplier tubes (PMT) and the noise level in selected samples can be comparable or better. However, it is often required to measure the fluorescence lifetime also, since it can provide useful information about conformational dynamics

[1]–[4], excited state energy transfer [5], and identification of individual molecules [6]–[8]. This is a challenging task, since various lifetime components of the fluorescent decay of a molecule can be very short, in the range of tens of picoseconds, especially when the fluorescence of the molecule is under a certain kind of quenching [1]–[4]. Hence, for identifying molecules or characterizing their dynamics on very short time scales, such as excited electron transfer or fluorescence resonance energy transfer (FRET), high time resolution is required together with high detection efficiency and low noise. In particular, new methods, devised by Yang and Xie [9], for extracting information about the conformational dynamics of the molecule and based on a statistical analysis of single-molecule fluorescence lifetime trajectories essentially rely on the availability of a detector with adequate performance: 1) better than 100-ps full-width at half-maximum (FWHM) of the time resolution function; 2) better than 30% QE in the wavelength range from 440 to 550 nm; and 3) less than 50 c/s dark counting rate. The available single-photon detectors based on fast PMTs can attain better than 100-ps FWHM resolution, but they have inadequate QE because of the intrinsic limits of the photocathodes. The commercially available single-photon counting modules (SPCM-AQR) by PerkinElmer (PKI) based on the SLIK silicon avalanche diode detector [10] have very good QE and low noise, but they have inadequate time resolution. In fact, the typical FWHM value of the SPCM-AQR is 350 ps and the intrinsic limit of SLIK devices, which can be attained operating the detector with different circuits, lies between 220 and 150 ps [11], [12]. However, a different avalanche device structure fabricated in planar silicon technology [13] offered a good prospect for the development of a single-photon timing module (SPTM) capable of fulfilling all the requirements. This goal has been attained: it has made accessible new information about angstrom-scale structural changes in single protein molecules, previously not obtained with other methods, and has made possible a correlation analysis of the fluorescence lifetime that revealed conformational fluctuation at multiple time scales spanning from hundreds of microseconds to seconds [3]. The work leading to the development of the SPTM is reported here.

## II. SPAD DEVICES AND QUENCHING CIRCUITS

The p-n junction diodes that can operate biased above the breakdown voltage $V_{BD}$ and generate macroscopic avalanche current pulses in response to single photons are called single-photon avalanche diodes (SPAD). The amount $V_E$ by which the applied bias voltage $V_A$ exceeds $V_{BD}$ is called

excess bias voltage ($V_E = V_A - V_{BD}$). The operation is radically different from that of the ordinary avalanche photodiodes (APDs), which are biased near to $V_{BD}$, but below it. It is instead similar to that of the Geiger–Muller counters of ionizing radiation; hence, SPADs are also quoted as Geiger-mode avalanche diodes. When a SPAD is biased at operative level the diode current is practically nil for a considerably long time (from hundreds of nanoseconds to many milliseconds) until a charge carrier is generated and succeeds in triggering the avalanche process. If the carrier is generated by a photon, the onset of the avalanche current marks the photon arrival time and can be sensed by a fast discriminator. The avalanche current flows until an external circuit quenches it by lowering the bias voltage to $V_{BD}$ or below. A dead-time follows; the bias is then restored and the photodiode is ready to detect the arrival of another photon. The passive-quenching circuit (consisting essentially in a high ballast resistor in series with the SPAD) is a simple solution but sets limitations to the maximum photon-counting rate and to the overall detector performance [12], [14]. Modern circuit technologies (up to monolithic integration of detector and ballast resistor) can make the recovery transient faster by reducing the stray capacitance and thus reduce the drawbacks, but they do not eliminate them. The solution that completely avoids these drawbacks is the active quenching circuit (AQC), first devised in 1975 [15], [16]. The AQC senses the leading edge of the avalanche current; it generates a standard output pulse, synchronous with the current onset; it quenches the avalanche by lowering the detector bias below the breakdown voltage; and it restores the photodiode voltage to the operative level after a well-defined hold-off time. In operation with an AQC, a SPAD works in accurately controlled bias conditions and the dead time following each pulse can be very short.

The main features and issues of the available silicon SPAD devices are here briefly summarized; more extensive descriptions and comparisons can be found elsewhere [14]. SLIK devices employed as SPAD in the SPCM-AQR by PKI are built in special ultra-pure high-resistivity silicon wafers with a dedicated and proprietary technological process [10]. The device structure with a thick depletion layer (about 30 $\mu$m) provides very good QE (better than 50% from 540 to 850 nm wavelength) but requires very high operating voltage (typically 400 V), produces high power dissipation during the avalanche (about 8 W), and limits the photon-timing resolution as quoted in Section I. A fairly wide active area (diameter about 170 $\mu$m) is obtained with low dark-counting rate, which is typically a few kc/s with the device at room temperature and is reduced in operation by cooling with a Peltier thermoelectric cooler (TEC).

A different approach to SPAD development was taken at our laboratory. SPAD devices were designed to operate with low voltage and low-power dissipation and developed in planar technologies compatible with the fabrication of integrated circuits and capable of producing rugged and reliable detector devices. Fig. 1 outlines the basic epitaxial structure introduced in 1988 [13] and developed in various technologies [17], [18]. The breakdown voltage $V_{BD}$ is typically 20 V and the depletion layer is typically 1 $\mu$m thick. By tailoring the epistrate thickness and the doping profile, the electric field profile can
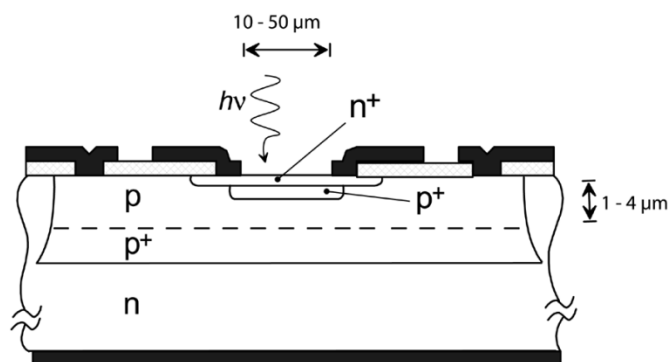


Fig. 1. Schematic cross section of the planar epitaxial SPAD employed.

be shaped and $V_{BD}$ can be adjusted in a range from 15 to 50 V. The optimization of the various parameters that characterize the detector performance set conflicting requirements to the design of the device structure and to the selection of operating conditions. Tradeoffs must be thoroughly evaluated.

The quantum detection efficiency (QE) depends on the probability that a photon be absorbed in the detector active volume and generates a primary electron-hole pair, as in other photodetectors. However, in SPADs it also depends on the probability that the primary carrier succeeds in triggering an avalanche, which is enhanced by a higher electric field. Hence, the QE depends on the electric field profile and increases with the excess bias voltage $V_E$ [12], [14].

The thermal generation of free carriers produces a dark-counting pulse rate and its poissonian fluctuations are the internal noise source of the detector. The dark-counting rate increases with the electric field and hence with $V_E$, not only because of the rise of the avalanche initiation probability, but also because some effects due to the electric field enhance the rate of generation of carriers [14]. Cooling can significantly reduce the generation rate in silicon (by about a factor two every 8 °C), but also in this respect a high electric field is detrimental since the rate of decrease of the dark-counting rate with temperature reduces with increasing electric field. The noise is further enhanced by a peculiar effect in SPADs. During each avalanche pulse, a few avalanche carriers are trapped in local deep levels at intermediate energy between mid-gap and band edge. They are subsequently released and can retrigger the avalanche, thereby generating correlated afterpulses [12], [14], [19]. The afterpulsing can be reduced by making the hold-off time of the AQC long enough to cover most of the delayed release events [12]. However, since the delay increases as the temperature decreases [19], at very low temperatures the necessary deadtime may become fairly long. For obtaining low noise, the key issue is to include in the fabrication process of the device suitable gettering steps that can very significantly reduce both generation centers and deep levels; careful design of the field profile in the device and selection of the operating conditions also contribute to reduce the detector noise [14].

The time resolution function of the planar epitaxial SPAD (i.e., the statistical distribution of the delays from the arrival time of the photon to the onset of the current pulse) has a fast peak followed by a slow tail [13], [14]. The peak is due to
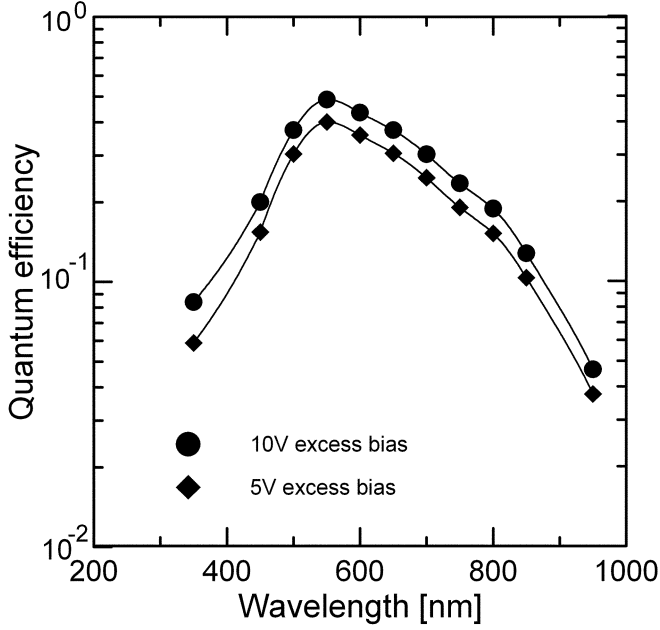
Fig. 2. QE of the planar SPAD employed, measured at excess bias values 5 and 10 V.
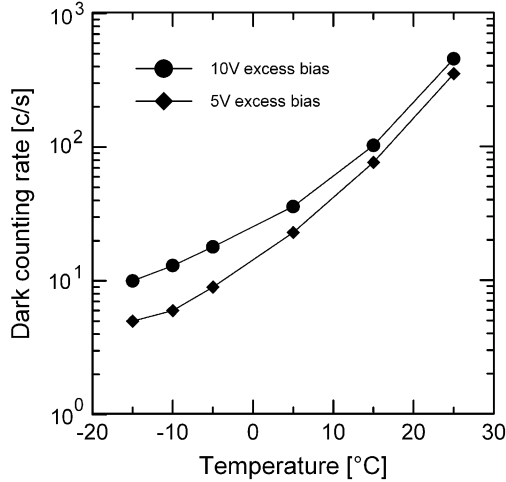


Fig. 3. Dark-counting rate versus temperature of the planar SPAD employed, measured at excess bias values 5 and 10 V.

photons absorbed in the depletion layer and its width is related to the statistical fluctuations in the avalanche build-up and in the propagation from the location of arrival of the photon to the whole active area [14], [20]. High electric fields reduce these fluctuations and FWHM values better than 30 ps have been obtained [14]. The tail is due to the minority carriers photogenerated in the neutral region beneath the junction that succeed in reaching the depletion region by diffusion and trigger the avalanche [13], [14], [21].

In the selection of planar SPAD devices for the required task, the performance tradeoff was established by accepting a nonoptimal FWHM resolution, but better than 100 ps, and seeking minimum noise and good QE. The selected devices had breakdown voltage about $V_{BD} = 26$ V at room temperature. Fig. 2 reports the QE measured at two different values of $V_E$. The dark-counting rate was measured at the same values of $V_E$ and its dependence on the temperature is illustrated in Fig. 3.
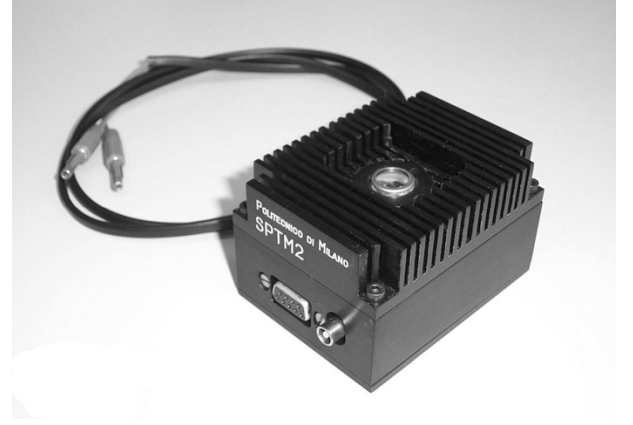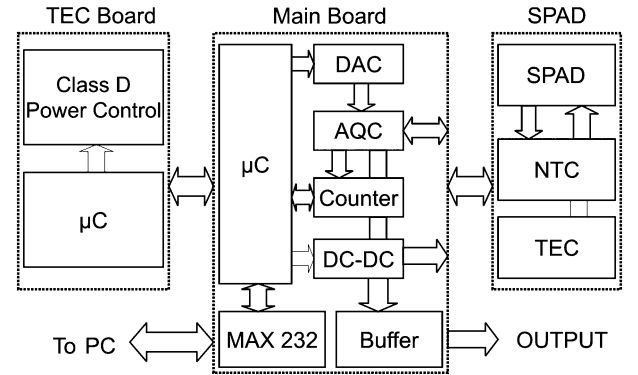


Fig. 4. View of the SPTM module.



Fig. 5. Schematic block diagram of the SPTM module.

## III. SPTM

The objective of the design was to obtain a compact and versatile module, including all the electronic circuitry necessary for exploiting the detector performance, relying on a single external standard voltage supply and able to operate with different samples of planar SPAD. The main operating parameters of the SPAD detector (excess bias voltage, hold-off time, and temperature) had to be adjustable under computer control, in order to easily fit the specific requirements in different applications (e.g., operation with the lowest dark counting rate or the highest photon-timing resolution). Furthermore, in order to be able to automate optical alignments, the photon-counting rate had to be directly monitored by the computer. The compact module ($82 \times 60 \times 30$ mm) developed is shown in Fig. 4. Its block diagram is illustrated in Fig. 5, and brief comments are given about its main blocks and functions.

### A. i-AQC

The SPTM employs a completely integrated i-AQC, which is the first monolithic circuit of this kind ever reported and is covered by U.S. and European patents [22], [23]. The i-AQC can operate with any available SPAD device, since it generates pulses high enough to quench SPADs operating with up to 30 V excess bias voltage. The dead time after the detection of a photon (which is the sum of the quenching delay plus an adjustable hold-off time plus the reset time) is adjustable and has a minimum value of 50 ns, corresponding to 20 Mcounts/s

maximum saturated photon-counting rate. Shrinking the circuit to a single chip with very low power dissipation (20 mW stand by, suitable also for portable instruments) has made it possible to design a really compact module. Since the planar SPAD detector also has low-power dissipation and is a very rugged device, the SPTM can be exposed to full ambient light without suffering any damage, thus making it simpler and easier to assemble and test new setups.

### B. Interfaces for Computer Control

A standard integrated circuit (MAX232) converts the RS-232 voltage levels from the computer to standard TTL signals. These signals are read by a Microchip PIC16F84 microcontroller ($\mu$C), which controls various blocks in the SPTM: the dc–dc converters that provide the internal supply voltages; the digital-to-analog converter (DAC) employed for setting the hold-off time value; and a custom integrated pulse counter. A separate circuit board contains a second microcontroller (Microchip PIC16F86), which implements a class D temperature controller. This board is independent and may be omitted in cases where the temperature control is not required, making possible a further reduction of the size of the module.

### C. Regulation of the SPAD Bias Voltage

Starting from the external power supply, the detector bias voltage is internally generated by means of a controlled dc–dc boost converter. A current-limited pulse frequency modulation (PFM) control scheme provides high-conversion efficiency. The fairly high switching frequency (up to 300 kHz) makes it possible to employ components of small size (transformer, etc.). The SPAD bias voltage can be finely adjusted from 18 to 43 V in steps of 300 mV. The bias voltage is set by the PC via the serial connection and can be stored in a memory within the SPTM for stand-alone operation. With the selected silicon planar SPAD devices employed, good signal-to-noise ratio in the photon detection is obtained operating with excess bias voltage in the range from 5 to 14 V. Accordingly, the supply voltage of the i-AQC has been set to +15 V, since this supply voltage sets a limit to the maximum excess bias voltage [22].

### D. Regulation of the Dead Time

The dead time is adjusted by digitally programming the hold-off time. The PIC16F84 microcontroller reads the value communicated by the PC via the RS-232 connection and by means of a DAC (MAX7224) supplies to the i-AQC a voltage, which sets the dead time value. This value can be selected from a minimum of 50 ns up to about 500 ns and can be stored in a nonvolatile RAM within the SPTM for stand-alone operation.

### E. SPAD Cooling and Temperature Regulation

The SPAD chip is housed in a standard TO8 case, glued onto a thermoelectric cooler (TEC), namely a two-stage Peltier element (part 2OT 1.4-24-F9 from Melcor). A glass-coated 1-k$\Omega$ thermistor (NTC, type 151-136, RS-Components) is glued directly on the SPAD chip. The glass window of the TO8 case is sealed in a nitrogen atmosphere. For maintaining the selected temperature value with a precision of $\pm$ 0.1 °C, a totally programmable class D digital temperature controller employing a proportional scheme was developed.

### F. Monitor of the Photon-Counting Rate

An ultra-compact counter microsystem is integrated in the same chip of the i-AQC and exploited for a continuous monitoring of the photon-counting rate. The system includes a 16-BIT CMOS counter, a 16-bit latch, a shift register, and control logic. The counter collects the pulses from the AQC in counting time intervals of 10 ms, set with high precision by the crystal-controlled timer of the microcontroller. At the end of each 10 ms interval, a fast logic signal from the microcontroller stops the counter. The accumulated count number is transferred to the register via the latch and the counter is then reset. The transfer and reset operations are not controlled by the microcontroller, but by the internal logic in the integrated counter system. Thanks to this feature, the dead time between two counting intervals is reduced to less than 40 ns. During the following 10-ms counting time, the data stored in the register are transferred by the microcontroller to the PC via the RS-232 connection. The maximum number of photon counts that can be accumulated during each 10-ms interval is 65536, which corresponds to a maximum counting rate of 6.5 Mcounts/s, a value more than adequate for all the envisaged counting applications. The serial port is configured to operate in low byte condition: 9600 baud, no parity, eight data bits, one stop bit. The PC classifies the count data in programmed time windows that can have duration from 10 ms to any desired multiple of it. A dedicated LabView software generates a plot of the waveform of counting rate versus time. The feature can be used for simplifying precise alignments in optical setups and for automating the alignment procedure.

### G. Preliminary Evaluation of the Performance

Preliminary tests of the performance of the SPTM with the selected SPAD sample were carried out on the bench, before employing it in the single-molecule experiments. The operating temperature of the SPAD was set at −15 °C and the dark-counting rate was checked to be 5 c/s with +5 V of excess bias voltage and 10 c/s with +10 V. The time resolution was measured with a standard time-correlated single photon counting (TCSPC) setup, with a time to amplitude converter (TAC) and a multichannel analyzer (MCA). A pulsed laser diode that generated light pulses at 820-nm wavelength with about 10-ps duration and 10-kHz repetition rate was employed. The FWHM of the measured histogram was 60 ps with SPAD operating at +10 V excess bias voltage and illumination focused on a small spot within the active area of the detector, as in the case of single molecule measurements. With uniform illumination of the whole active area the FWHM was better than 100 ps. With +5 V of excess bias voltage the FWHM values were 80 ps with focused illumination and 125 ps with uniform illumination.
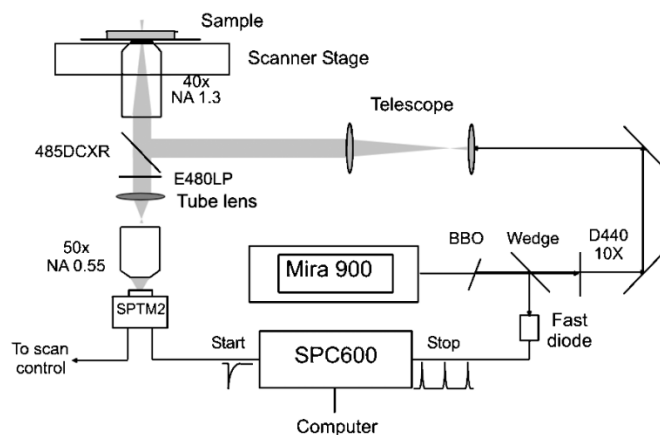
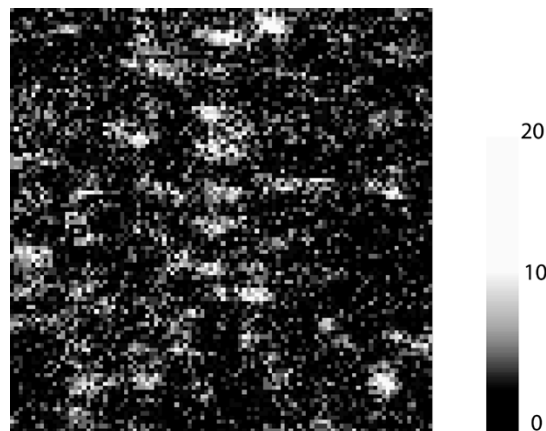Fig. 6. Experimental setup for single molecule lifetime measurements.



Fig. 7. Fluorescence image of individual molecules of Alexa fluor 430 (Molecular Probes) spin-coated onto the quartz surface, as obtained by scanning and photon-rate measurements.

## IV. SINGLE-MOLECULE MEASUREMENTS

### A. Experimental Setup

The experimental setup for the single molecule lifetime measurements with the SPTM is shown in Fig. 6. A frequency-doubled Coherent Mira 900 F Ti: Sapphire laser is used to provide the excitation pulses with a wavelength of 440 nm and a repetition rate of 76 MHz. The collimated excitation beam was directed into an inverted microscope (AxioVert 135, Zeiss) by a dichroic beam splitter (485DCXR, Chroma) and then focused onto the sample via a NA 1.3 oil-immersion objective lens (Fluar 40X, Zeiss). The same objective was used to collect the fluorescence or the back reflection of the laser. The fluorescence, passing through the tube lens, was spectrally filtered by a dielectric long-pass filter (E480LP, Chroma). After the first imaging plane (the focal plane of the tube lens), the diverging fluorescence beam was refocused by an 8.2-mm working distance, 50X objective (0.55 NA, Nikon) into the 20-$\mu$m active area of the SPAD. The optical setup is optimized for the detection of single molecule fluorescence with the SPTM. Since the active area of the SPAD is very small, an objective with low magnification (40X) in the illumination part as well as a long working distance objective in the collection part is used to reduce the size of the fluorescence image. Therefore, most of the fluorescence collected by the 40X objective is directed into the small active area of the detector, thus maximizing the detection efficiency. Imaging the sample with a high magnification objective (100X) would cause severe loss of the fluorescence signal and make the setup not useful for single molecule detection, because most of the fluorescence would be focused outside the detector active area. For the same reason, the long working distance objective with high NA in the collection part is also necessary.

The first phase of the experiments consists of finding the locations of immobilized single molecules on the surface of a quartz plate. By scanning the surface and recording the detected photon rate a fluorescence image is obtained. A good signal-to-background ratio is crucial for detecting the fluorescence signal from an individual molecule. In order to collect as much fluorescence from the target molecule as possible and reject the out-of-focus background signal, the fluorescence spot size must match the

size of the detector active area. Care is taken to adjust the $z$ position of the refocusing objective with respect to the first imaging plane so that the actual size of the fluorescence spot can be adjusted as well. After this optimization, the confocal microscope is capable of imaging the immobilized single fluorescence molecules. Fig. 7 shows a demonstrative example where the signal-to-background ratio obtained can be considered good, given the low absorption cross section (15000 cm$^{-1}$M$^{-1}$) and the low quantum efficiency of the dye (about 10%, estimated from lifetime measurements).

In the fluorescence decay measurements, the detected photon signal given by the SPTM triggers the start of the time-to-amplitude conversion (TAC) in reversed counting mode. A fast photodiode is used to obtain the excitation pulse signal, which serves as the stop signal of the TAC. A time correlated single-photon counting (TCSPC) card (SPC-600, Becker & Hickl) is used to record the fluorescence decay histogram; both the delay with respect to the excitation pulse and the chronological time can be recorded for each detected photon [3], [9]. The TCSPC data are recorded in 4096 channels within a 12.5-ns time window, corresponding to 3 ps per channel.

### B. Sample Preparation

For testing the SPTM in single-molecule lifetime measurements, a single complex of NAD(P)H : flavin oxidoreductase (Fre) and flavin adenine dinucleotide (FAD) was selected. The Fre–FAD complex was tethered onto the surface of quartz with a biotin-streptavidin linker12. Briefly, the Fre is labeled by an amide formation reaction between the amino groups of Fre and biotin-(PEG)-succinimidyl ester (Shearwater Polymers). To prepare a streptavidin coated surface, a hydrophilic quartz coverslip was first immersed in the 1.0 mg·mL-1 biotinated BSA solution and then was treated with the 0.2 mg·mL-1 streptavidin solution. The enzyme was linked to the surface by absorbing 10-nM biotinated-Fre onto the streptavidin coated quartz coverslip. Finally, the coverslip was immersed in the 2-$\mu$M FAD solution. Between two incubations, the surface is rinsed with a 20-mM phosphate buffer. The immobilized Fre–FAD sample was then imaged under the 20-mM phosphate buffer with the confocal fluorescence microscope.
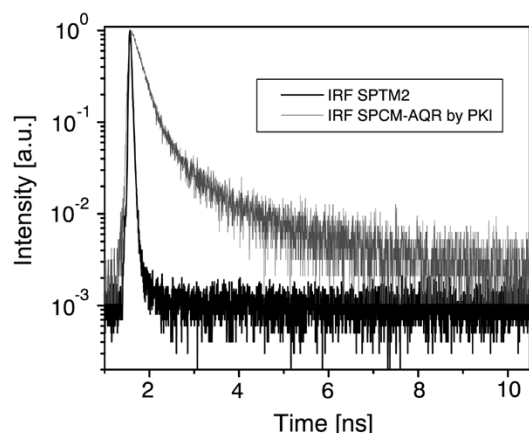
Fig. 8. Instrumental time response function of the system obtained with a SPTM compared to that obtained with a PerkinElmer SPCM-AQR in the same setup.
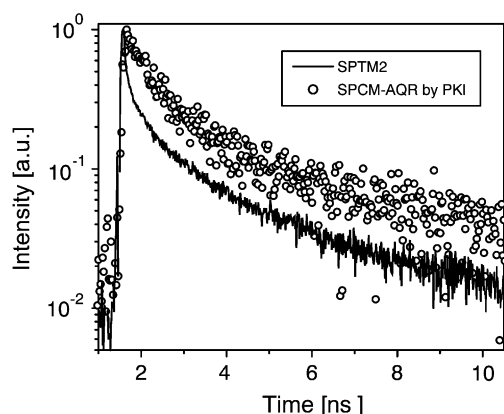


Fig. 9. Fluorescence decay histogram of a single Fre–FAD complex measured with the SPTM (solid line). For comparison, the histogram measured with a PerkinElmer SPCM-AQR in the same setup is also reported (circles).

## C. Results and Discussion

Comparative tests were made employing the SPTM prototype and an SPCM-AQR by PKI in the experimental setup. First, a direct comparison of the absolute fluorescence signals obtained from bulk sample confirmed that in the wavelength range from 440 to 550 nm the two detectors have similar detection efficiency. The instrumental response function (IRF) of the system was then measured by detecting the back-reflected laser pulse. As illustrated in Fig. 8, the IRF obtained with the SPTM has 62-ps FWHM and provides a remarkable improvement of the time resolution with respect to the SPCM-AQR. In this case, the slow exponential diffusion tail of the IRF (see Section II) is not present, because all photons with 440-nm wavelength are absorbed within the depletion layer. Also, with illumination at longer wavelengths the well-behaved shape of the IRF makes it possible to resolve fluorescence components with lifetime down to one-fifth of the FWHM of the IRF, as reported by Louis *et al.* [24]. The sharpness of the time response depends on the alignment of the system. The best response is obtained by carefully aligning the lighted spot to the center of the active area. A misaligned or defocused beam causes the FWHM to increase to about 90 ps. The effect is well known and depends on the

physical phenomena associated with the statistical propagation of the avalanche current from the initial location of incidence of the photon to the whole active area of the detector [20].

In Fig. 9, the measured histograms of the fluorescence decay of a single Fre–FAD complex are shown. In the histogram obtained with the SPTM, the decay can be fitted by three lifetime components, with lifetimes and relative populations of 79.1 ps (73.1%), 386 ps (13.6%), and 1.43 ns (13.2%), respectively. Clearly, in the histogram obtained with the SPCM-AQR the short lifetime component cannot be well resolved. The higher accuracy provided by the SPTM in the measurement of the short lifetime components makes it possible to determine more accurately the single molecule lifetime probability distribution. Furthermore, the faster time response of the SPTM makes it possible to reduce more effectively the background by means of the lifetime gating [7], [25]. In fact, in cases where the Raman signal is the major background source in the single molecule experiment, the background level can be reduced to 1/20 without losing any fluorescence signal.

## V. CONCLUSION

The combination of high time resolution, high detection efficiency, and low dark-counting rate of the SPTM makes it possible to measure the fluorescent decay of a single molecule even with very short lifetime. Resolving short lifetime components is important in many cases. In measurements obtained with detectors of lower time resolution, the convolution with a wider instrumental response can hide short lifetime components even if they have high population. In the single molecule studies, high time resolution makes it possible to probe broader conformational distribution in a system where the fluorescence can be quenched by electron transfer (ET) [3] or fluorescence resonance energy transfer (FRET) [5], [8]. In the Fre–FAD complex the fluorescence of the isoalloxazine chromophore is quenched by the nearby tyrosine through excited state electron transfer [16], [17]. Because the enzyme undergoes continuous conformational fluctuation, the change of the quenching rate due to the fluctuation of chromophore and quencher distance will result in multiple lifetime components of the single-molecule fluorescence decay. As reported elsewhere [3], the SPTM has made it possible to probe the fluorescence lifetime of the single flavin on a photon-by-photon basis, hence to observe the variation of flavine–tyrosine distance over time and to carry out a correlation analysis that revealed conformational fluctuations of the molecule at multiple time scales spanning from hundreds of microseconds to seconds.

## REFERENCES

[1] L. Edman, U. Mets, and R. Rigler, "Conformational transitions monitored for single molecules in solution," in *Proc. Nat. Acad. Sci. USA*, vol. 93, 1996, pp. 6710–6715.

[2] Y. Jia, A. Sytnik, L. Li, S. Vladimirov, B. S. Cooperman, and R. M. Hochstrasser, "Nonexponential kinetics of a single tRNA$^{Phe}$ molecule under physiological conditions," in *Proc. Nat. Acad. Sci. USA*, vol. 94, 1997, pp. 7932–7936.

[3] H. Yang, G. Luo, P. Karnchanaphanurach, T.-M. Louie, I. Rech, S. Cova, L. Xun, and X. S. Xie, "Protein conformational dynamics probed by single-molecule electron transfer," *Science*, vol. 302, pp. 262–266, 2003.

[4] C. Eggeling, J. R. Fries, L. Brand, R. Gunther, and C. A. Seidel, "Monitoring conformational dynamics of a single molecule by selective fluorescence spectroscopy," in *Proc. Nat. Acad. Sci. USA*, vol. 95, 1998, pp. 1556–1561.

[5] F. Kohn, J. Hofkens, R. Gronheid, M. Cotlet, K. Mullen, M. Van der Auweraer, and F. C. De Schryver, "Excitation energy transfer in dendritic host-guest donor-acceptor systems," *F. C. Chem. Phys. Chem.*, vol. 3, pp. 1005–1013, 2002.

[6] M. Sauer, J. Arden-Jacob, K. H. Drexhage, F. Göbel, U. Lieberwirth, K. Mühlegger, R. Müller, and J. Wolfrum, "Time-resolved identification of individual mononucleotide molecules in aqueous solution with pulsed semiconductor lasers," *C. Bioimaging*, vol. 6, pp. 14–24, 1998.

[7] C. Eggeling, S. Berger, L. Brand, J. R. Fries, J. Schaffer, A. Volkmer, and C. A. Seidel, "Data registration and selective analysis for single-molecule fluorescence spectroscopy using BIFL," *J. Biotechnol.*, vol. 86, pp. 163–180, 2001.

[8] M. Cotlet, J. Hofkens, S. Habuchi, G. Dirix, M. Van Guyse, J. Michiels, J. Vanderleyden, and F. C. De Schryver, "Identification of different emitting species in the red fluorescent protein DsRed by means of ensemble and single-molecule spectroscopy," in *Proc. Nat. Acad. Sci. USA*, vol. 98, 2001, pp. 14 398–14 403.

[9] H. Yang and X. S. Xie, "Probing singler-molecule dynamics photon by photon," *J. Chem. Phys.*, vol. 117, pp. 10 965–10 979, 2002.

[10] H. Dautet, P. Deschamps, B. Dion, A. D. MacGregor, D. MacSween, R. J. McIntyre, C. Trottier, and P. P. Webb, "Photon counting techniques with silicon avalanche photodiodes," *Appl. Opt.*, vol. 32, pp. 3894–3900, 1993.

[11] L. Q. Li and L. M. Davis, "Single photon avalanche diode for single molecule detection," *Rev. Sci. Instrum.*, vol. 64, pp. 1524–1529, 1993.

[12] S. Cova, M. Ghioni, A. Lacaita, C. Samori, and F. Zappa, "Avalanche photodiodes and quenching circuits for single photon detection," *Appl. Opt.*, vol. 35, pp. 1956–1976, 1996.

[13] A. Lacaita, M. Ghioni, and S. Cova, "Double epitaxy improves single-photon avalanche diode performance," *Electron. Lett.*, vol. 25, pp. 841–843, 1989.

[14] S. Cova, M. Ghioni, A. Lotito, I. Rech, and F. Zappa, Evolution and prospect of single-photon avalanche diodes and quenching circuits, in *NIST-ARDA Workshop Single-Photon Detectors*, Gaithersburg, MD, Mar. 31–Apr. 1 2003.

[15] P. Antognetti, S. Cova, and A. Longoni, "A study of the operation and performances of an avalanche diode as a single photon detector," in *Proc. 2nd Ispra Nuclear Electronics Symp.*, Stresa, Italy, May 20–23, 1975. Euratom EUR 537e, 453-456.

[16] S. Cova, A. Longoni, and A. Andreoni, "Toward picosecond resolution with single-photon avalanche diodes," *Rev. Sci. Instrum.*, vol. 52, pp. 408–412, 1981.

[17] F. Zappa, M. Ghioni, S. Cova, L. Varisco, B. Sinnis, A. Morrison, and A. Mathewson, "Integrated array of avalanche photodiodes for single photon counting," in *Proc. Eur. Solid State Device Res. Conf.*, Stuttgart, Germany, Sept. 22–24, 1997. ESSDERC97, 600-603.

[18] E. Sciacca, A. Giudice, D. Sanfilippo, F. Zappa, S. Lombardo, R. Consentino, C. Di Franco, M. Ghioni, G. Fallica, G. Bonanno, S. Cova, and E. Rimini, "Silicon planar technology for single-photon optical detectors," *IEEE Trans. Electron Devices*, vol. 50, pp. 918–925, 2003.

[19] S. Cova, A. Lacaita, and G. Ripamonti, "Trapping phenomena in avalanche photodiodes on nanosecond scale," *IEEE Trans. Electron. Device Lett.*, vol. 12, pp. 685–687, 1991.

[20] A. Lacaita and M. Mastrapasqua, "Strong dependence of time resolution on detector diameter in single photon avalanche diodes," *Electron. Lett.*, vol. 26, pp. 2053–2054, 1990.

[21] G. Ripamonti and S. Cova, "Carrier diffusion effects in the time-response of a fast photodiode," *Solid State Electron.*, vol. 28, pp. 925–931, 1985.

[22] F. Zappa, A. Lotito, A. C. Giudice, S. Cova, and M. Ghioni, "Monolithic active-quenching and active-reset circuit for single-photon avalanche detectors," *IEEE J. Solid-State Circuits*, vol. 38, pp. 1298–1301, 2003.

[23] F. Zappa, S. Cova, and M. Ghioni, "Monolithic circuit of active quenching and active reset for avalanche photodiodes,". Eur. Pat. Appl. n. 01 200 852.2-2217, Mar. 6, 2001.

[24] T. A. Louis, G. H. Schatz, P. Klein-Bolting, A. R. Holzwarth, G. Ripamonti, and S. Cova, "Performance comparison of a single-photon avalanche diode with a microchannel-plate photomultiplier in time-correlated single-photon counting," *Rev. Sci. Instrum.*, vol. 59, pp. 1148–1152, 1988.

[25] S. A. Soper, L. M. Davis, and E. B. Shera, "Detection and identification of single molecules in solution," *J. Opt. Soc. Amer. B*, vol. 9, pp. 1761–1769, 1992.
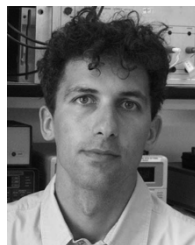
**Ivan Rech** was born in Milan, Italy, in 1976. He received the B.S. degree in electronics engineering from the Politecnico di Milano, Milan, in 2000, where he is currently working toward the Ph.D. degree in electronics and communications in the research group of Prof. S. Cova.

His research interests include the development of single-photon measurement systems for biological applications (DNA and protein analysis).


**Guobin Luo** received the B.S. degree in chemistry from Zhongshan University, China, in 1997 and the M.S. degree in physical chemistry from Peking University, Peking, China, in 2000. He is currently working toward the Ph.D. degree in the Department of Chemistry and Chemical Biology, Harvard University, Cambridge, MA, in the research group of Prof. S. Xie.

His research interests include single-molecule fluorescence measurements to study the dynamics of biomacromolecules.
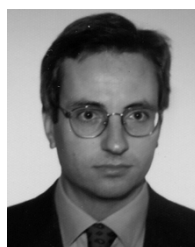

**Massimo Ghioni** (M'91) was born in 1962 in Monza, Italy. He received the B.S. degree in nuclear engineering from the Politecnico di Milano, Milan, Italy, in 1987.

He is a Full Professor of Electronics with the Department of Electronics and Information Science, Politecnico di Milano. In 1992, he was a Visiting Scientist at the IBM T. J. Watson Research Center, Yorktown Heights, NY, where he worked on silicon photodetectors for integrated optical receivers. His current research interests include the study and development of single-photon detectors and associated electronics for scientific and industrial applications, such as advanced microanalytical techniques for medical diagnostic applications (DNA and protein analysis), adaptive optical systems for astronomy, and quantum cryptography.


**Haw Yang** received the B.S. degree in chemistry from the National Taiwan University, Taipei, Taiwan, R.O.C., in 1991 and the Ph.D. degree in physical chemistry from the University of California, Berkeley, in 1999.

After completing his post-doctoral research at Harvard University, Cambridge, MA, in 2002, he joined the Faculty of the University of California, Berkeley, where he is currently an Assistant Professor of chemistry. His recent research interests include development of spectroscopic techniques to study the behavior of individual biological macromolecules.

Dr. Yang is a member of the American Physics Society, the American Chemical Society, the Biophysical Society, and the American Association for the Advancement of Science.

**Xiaoliang Sunney Xie** received the Ph.D. degree in chemistry from the University of California, San Diego, in 1990, after which he did postdoctoral work at the University of Chicago.

He is a Professor of Chemistry in the Department of Chemistry and Chemical Biology, Harvard University, Cambridge, MA. In 1992, he joined the Pacific Northwest National Laboratory as a Senior Research Scientist, and in 1995 was appointed Chief Scientist for their Environmental Molecular Sciences Laboratory. He joined the Harvard faculty as a Full Professor in 1999. His research group helped to pioneer room-temperature fluorescence studies of single molecules and has since made significant advances in single-molecule enzymology. Other areas of investigation include real-time tracking of gene expression in live cells and the development of advanced spectroscopy and microscopy tools for bioimaging, notably coherent anti-Stokes Raman scattering (CARS) microscopy.

Dr. Xie was a recipient of the Coblentz Award in 1996 and the Sackler Prize in the Physical Sciences in 2003.

**Sergio Cova** (F'02) was born in Roma, Italy, in 1938. He received the Ph.D. degree in nuclear engineering in 1962 from Politecnico di Milano, Milan, Italy.

He has been a Full Professor of Electronics at the Politecnico di Milano since 1976. He is the author of over 150 papers in international refereed journals and conference proceedings and of five international patents (U.S. and Europe). He has given innovative contributions in the research and development of detectors for optical and ionising radiations and associated electronics, of microelectronic devices and circuits, and of electronic and optoelectronic measurement instrumentation and systems. He pioneered the development of single-photon avalanche diodes, inventing the active-quenching circuit AQC, which opened the way to their application, and devised new SPAD device structures. He has collaborated with interdisciplinary research in physics, astronomy, cytology, and molecular biology, developing dedicated electronic and optoelectronic devices and instrumentation.